Neuron
Article

Mechanism of Ca^{2+} Disruption in Alzheimer's Disease by Presenilin Regulation of $InsP_3$ Receptor Channel Gating

King-Ho Cheung,[1] Diana Shineman,[2,4] Marioly Müller,[1] César Cárdenas,[3] Lijuan Mei,[1] Jun Yang,[1] Taisuke Tomita,[5] Takeshi Iwatsubo,[5] Virginia M.-Y. Lee,[2,4] and J. Kevin Foskett[1,3,*]
[1]Department of Physiology
[2]Department of Pathology and Laboratory Medicine
[3]Department of Cell and Developmental Biology
[4]Center for Neurodegenerative Disease Research
University of Pennsylvania, Philadelphia, PA 19104, USA
[5]Department of Neuropathology and Neuroscience, University of Tokyo, Tokyo 113-0033, Japan
*Correspondence: foskett@mail.med.upenn.edu
DOI 10.1016/j.neuron.2008.04.015

SUMMARY

Mutations in presenilins (PS) are the major cause of familial Alzheimer's disease (FAD) and have been associated with calcium (Ca^{2+}) signaling abnormalities. Here, we demonstrate that FAD mutant PS1 (M146L) and PS2 (N141I) interact with the inositol 1,4,5-trisphosphate receptor ($InsP_3R$) Ca^{2+} release channel and exert profound stimulatory effects on its gating activity in response to saturating and suboptimal levels of $InsP_3$. These interactions result in exaggerated cellular Ca^{2+} signaling in response to agonist stimulation as well as enhanced low-level Ca^{2+} signaling in unstimulated cells. Parallel studies in $InsP_3R$-expressing and -deficient cells revealed that enhanced Ca^{2+} release from the endoplasmic reticulum as a result of the specific interaction of PS1-M146L with the $InsP_3R$ stimulates amyloid beta processing, an important feature of AD pathology. These observations provide molecular insights into the "Ca^{2+} dysregulation" hypothesis of AD pathogenesis and suggest novel targets for therapeutic intervention.

INTRODUCTION

Alzheimer's disease (AD) is a common dementia involving slowly developing and ultimately fatal neurodegeneration. Most AD is sporadic and usually develops at age >60, but ~10% of AD is inherited as an autosomal-dominant trait (familial AD, FAD) and disease develops as early as the late 30 years of age. Mutations in amyloid precursor protein (APP) and presenilins (PS1, PS2) cause early onset FAD (Hutton and Hardy, 1997). Hallmark features of AD include accumulations of extracellular β amyloid (Aβ) plaques and intracellular neurofibrillary tangles with neuronal atrophy or loss (Hardy, 2006; Mattson, 2004). The "amyloid hypothesis" of AD postulates that accumulation of oligomeric or fibrillar Aβ, due to production of more amyloidogenic forms of Aβ and defective processing and clearance, leads to pathological sequelae associated with the disease (Haass and Selkoe, 2007; Hardy and Selkoe, 2002). This hypothesis has nevertheless been questioned (De Strooper, 2007; Hardy and Selkoe, 2002; Shen and Kelleher, 2007), and others have also been proposed to describe pathological origins of the disease (reviewed in Blennow et al., 2006; Mattson, 2004). Accumulating evidence suggests that sustained disruption of intracellular Ca^{2+} signaling may play an early proximal, and perhaps central, role in AD pathogenesis (Gandy et al., 2006; LaFerla, 2002; Mattson and Chan, 2003; Smith et al., 2005a; Stutzmann, 2005). Ca^{2+} is involved in many facets of neuronal physiology, including activity, growth and differentiation, synaptic plasticity, and learning and memory, as well as pathophysiology, including necrosis, apoptosis, and degeneration (Berridge et al., 2000). Before identification of PS, Ito (Ito et al., 1994) discovered that fibroblast lines derived from AD patients, later shown to harbor the A246Q mutation in PS1, without exception, generated exaggerated intracellular Ca^{2+} concentration ($[Ca^{2+}]_i$) responses to submaximal concentrations of two G protein-coupled receptor (GPCR) agonists that activate phospholipase C (PLC). Activation of GPCR, including bradykinin, $5HT_{2A}$ and metabotropic glutamate receptors, stimulates PLC activity that produces inositol 1,4,5-trisphosphate ($InsP_3$), which binds to its receptor ($InsP_3R$), an endoplasmic reticulum (ER)-localized Ca^{2+} channel, resulting in release of Ca^{2+} from the ER and elevation of $[Ca^{2+}]_i$ (Foskett et al., 2007). Enhanced Ca^{2+} release could not be attributed to altered amounts of Ca^{2+} in the ER or number of agonist receptors or to plasma membrane influx pathways (Ito et al., 1994). It was suggested that alteration of $InsP_3R$-mediated Ca^{2+} release was a fundamental defect in AD, although the molecular mechanisms were undefined. Subsequently, it was demonstrated that enhanced $InsP_3$-mediated Ca^{2+} signaling was a highly predictive diagnostic feature of AD-derived peripheral cells (Hirashima et al., 1996). Many subsequent studies have confirmed that mutant PS expression is associated with exaggerated ER Ca^{2+} release in several cellular and animal model systems including cells from FAD patients (Etcheberrigaray et al., 1998; Hirashima et al.,

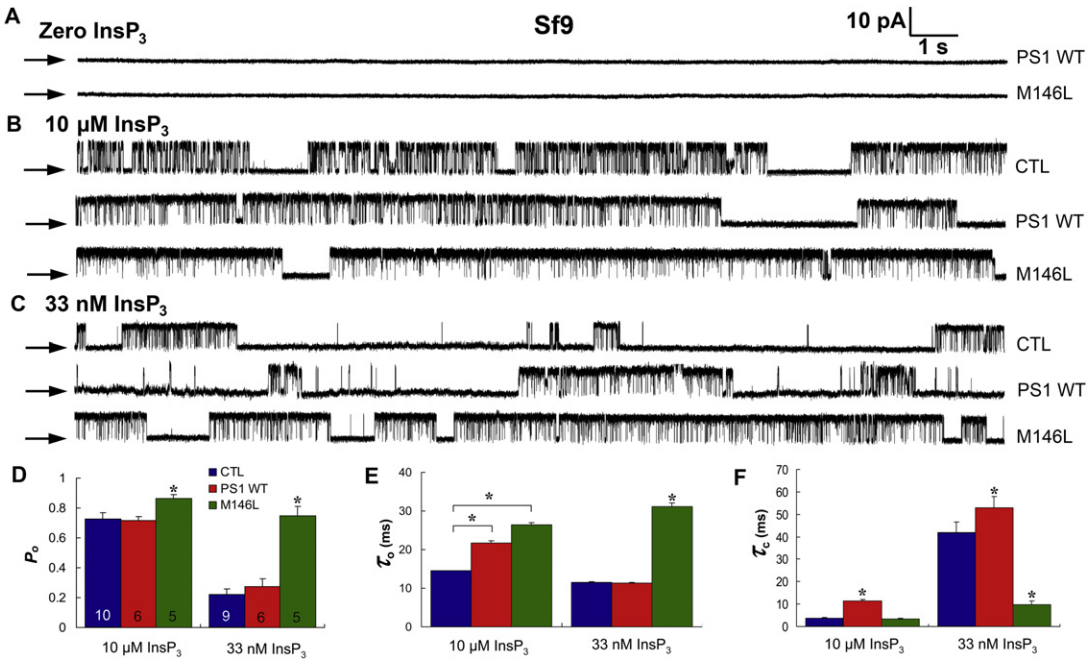

Figure 1. Effects of PS1 Expression on $InsP_3R$ Single-Channel Activity in Sf9 Cells

(A–C) Representative current recordings in isolated nuclei from Sf9 cells infected with PS1 WT or M146L baculoviruses in absence (A) or presence of saturating (10 μM; B) or subsaturating (33 nM; C) $InsP_3$ in pipette solution. Channel activity was not evoked by PS1 alone in absence of $InsP_3$ (A), whereas $InsP_3R$ channels were activated in presence of $InsP_3$ (B and C). Pipette [Ca^{2+}] was 1 μM; arrows: zero current level. Summary of effects of PS1 expression on $InsP_3R$ channel open probability P_o (D) mean open time (τ_o) (E) and mean closed time (τ_c) (F). Bars indicate standard error of the mean. Asterisks: $p < 0.01$, unpaired t test. Data presented in Table S1.

1996; Ito et al., 1994), neuronal and nonneuronal cells engineered to express recombinant mutant PS proteins (Cedazo-Minguez et al., 2002; Guo et al., 1996; Johnston et al., 2006; Leissring et al., 1999a, 1999b, 2001; Smith et al., 2002) and cells from mutant PS transgenic animals (Leissring et al., 2000), including brain neurons (Barrow et al., 2000; Mattson et al., 2000; Schneider et al., 2001; Stutzmann et al., 2004, 2006) long before the appearance of plaques and tangles (Stutzmann et al., 2004). A "Ca^{2+} overload" hypothesis has been widely invoked to account for exaggerated Ca^{2+} release in mutant PS-expressing cells (discussed in Stutzmann, 2005), but increased ER Ca^{2+} stores have not been consistently observed (Giacomello et al., 2005; Ito et al., 1994; Lessard et al., 2005; Zatti et al., 2004, 2006) nor is there a consensus regarding possible molecular mechanisms involved (Gandy et al., 2006; LaFerla, 2002; Smith et al., 2005a; Stutzmann, 2005). Here, we have discovered a mechanism that can account for intrinsic altered Ca^{2+} signaling in AD cells that involves a biochemical and functional interaction of WT and FAD mutant PS with the $InsP_3R$ Ca^{2+} release channel. The biochemical interactions of FAD mutant PS1 or PS2 with the $InsP_3R$ profoundly enhance the activity (gating) of the channel that results in and can account for exaggerated cellular Ca^{2+} signaling. By use of $InsP_3R$-deficient cells, we show that this enhancement is directly involved in mutant PS-mediated APP processing (Aβ generation), an important feature of AD pathology (Mattson and Guo, 1997).

RESULTS

Modulation of $InsP_3R$ Channel Activity by PS1 in Sf9 Cells

The effects of PS expression on $InsP_3R$ channel activity were examined in native ER membranes by single-channel patch-clamp electrophysiology of the outer membrane of isolated Sf9 cell nuclei (Ionescu et al., 2006). Insect cells express a single $InsP_3R$ isoform, most closely related to the mammalian type 1 channel, the predominant brain isoform (Foskett et al., 2007), that has permeation and gating properties and ligand regulation very similar to those of mammalian $InsP_3R$ channels (Ionescu et al., 2006). In membrane patches from control nuclei, $InsP_3R$ channels exposed to optimal ligand conditions (10 μM $InsP_3$, 1 μM Ca^{2+}) were consistently detected, and they gated with high open probability ($P_o = 0.76 \pm 0.05$, n = 10; Figure 1B and see Table S1 available online). Human wild-type PS1 (PS1-WT) and FAD mutant PS1 M146L (PS1-M146L) were expressed in Sf9 cells as full-length holoproteins (Figure S1) throughout the ER (not shown) and in the nuclear envelope (Figure S2). In nuclei from either FAD mutant PS1-M146L- or PS1-WT-expressing cells, no novel ion channels were detected (n = 59; Figure 1A). Nor were channel activities observed in the absence of $InsP_3$ (n = 10; Figure 1A) or in the presence of $InsP_3$ together with its competitive inhibitor heparin (100 μg/ml; n = 7; not shown). $InsP_3R$ channels observed in the presence of saturating 10 μM $InsP_3$ in membrane patches

from PS1-WT-infected cells had P_o similar to those from mock-infected or uninfected cells ($p > 0.05$; Figures 1B and 1D). In contrast, P_o was elevated ($p < 0.05$) in PS1-M146L-infected cells ($P_o = 0.86 \pm 0.03$; Figures 1B and 1D), with many channels observed to be "locked open" for long periods (as in Figure 1B), a gating behavior only extremely rarely observed in control channels (unpublished data). PS1-M146L enhanced $InsP_3R$ gating in saturating [$InsP_3$] by prolonging the channel open time (Figure 1E). Interestingly, PS1-WT also enhanced the mean open time, although to a lesser extent than mutant PS1 (Figure 1E), and it also enhanced the mean closed time (Figure 1F).

With [$InsP_3$] lowered to 33 nM, $InsP_3R$ channel P_o in patches from control nuclei was reduced to 0.27 ± 0.01, reflecting the [$InsP_3$] dependence of gating (Ionescu et al., 2006). Strikingly, P_o was elevated by nearly 3-fold in patches from nuclei isolated from the FAD mutant PS1-expressing cells ($P_o = 0.75 \pm 0.06$), to a level that was comparable to that observed in saturating [$InsP_3$] (Figures 1C and 1D). Enhanced P_o was caused by a marked destabilization of the channel closed state (enhanced opening rate) as well as prolongation of the open time (Figures 1E and 1F). In contrast, PS1-WT was without effect on P_o (Figure 1D); although it appeared to influence channel gating, reflected as a small increase of the channel mean closed time (Figure 1F).

Biochemical Interaction of PS1 with $InsP_3R$

These results demonstrate a gain-of-function effect of mutant PS1 on $InsP_3R$ channel activity observed at the single-channel level. Because the effects of FAD PS1 expression were observed in isolated nuclei, we speculated that this functional effect was caused by an association of PS with the $InsP_3R$ in the ER membrane patches. PS1-WT and PS1-M146L immunoprecipitates from Sf9 cells that had been co-infected with rat types 1 or 3 $InsP_3R$ contained both $InsP_3R$ channel isoforms (Figure 2A). Similarly, PS1 immunoprecipitates from mouse whole brain lysates contained the type 1 $InsP_3R$ (Figure 2C). These results demonstrate a biochemical interaction between $InsP_3R$ and both WT and mutant PS1.

Modulation of $InsP_3R$ Channel Activity by PS1 in DT40 Cells

Similar studies were undertaken in chicken DT40 cells, using analogous protocols, but with polyclonal lines engineered to stably express either WT or mutant PS1 proteins (Figure S3). A DT40 line with all three $InsP_3R$ isoforms genetically deleted ($InsP_3R$-KO DT40) constitutes the only $InsP_3R$ null cell line available (Sugawara et al., 1997). We reasoned that if PS1 similarly affected gating of $InsP_3R$ channels in native $InsP_3R$-expressing DT40 cells, the generality of this as a molecular mechanism associated with FAD mutant PS1 could be established, and furthermore that use of $InsP_3R$-KO DT40 cells would be valuable for investigating the physiological relevance of the PS-$InsP_3R$ interaction. As in the Sf9 cell recordings, no novel ion channel activities were observed in nuclei from the wild-type or mutant PS1-expressing native DT40 cells (not shown). Importantly, highly similar effects of PS expression on $InsP_3R$ channel behavior were observed as in the Sf9 cells (Figure 3; Table S2). Thus, in saturating [$InsP_3$], PS1-WT was without effect ($P_o = 0.53 \pm 0.05$ in control versus 0.57 ± 0.07 in PS1-WT transfected cells), whereas PS1-M146L expression increased channel activity ($P_o = 0.83 \pm 0.04$; $p < 0.01$; Figures 3A and 3C) by locking the channel open for long periods (Figure 3D). In suboptimal [$InsP_3$] (100 nM), mutant PS1 stimulated channel activity by 4-fold ($P_o = 0.63 \pm 0.07$ versus 0.16 ± 0.02 for control cells; Figures 3B and 3C) to levels similar to those observed for control channels in saturating [$InsP_3$]. Also as in Sf9 cells, PS1-WT was without effect on P_o, although it influenced channel gating, as evidenced by small effects on both mean open and closed times (Figures 3D and 3E).

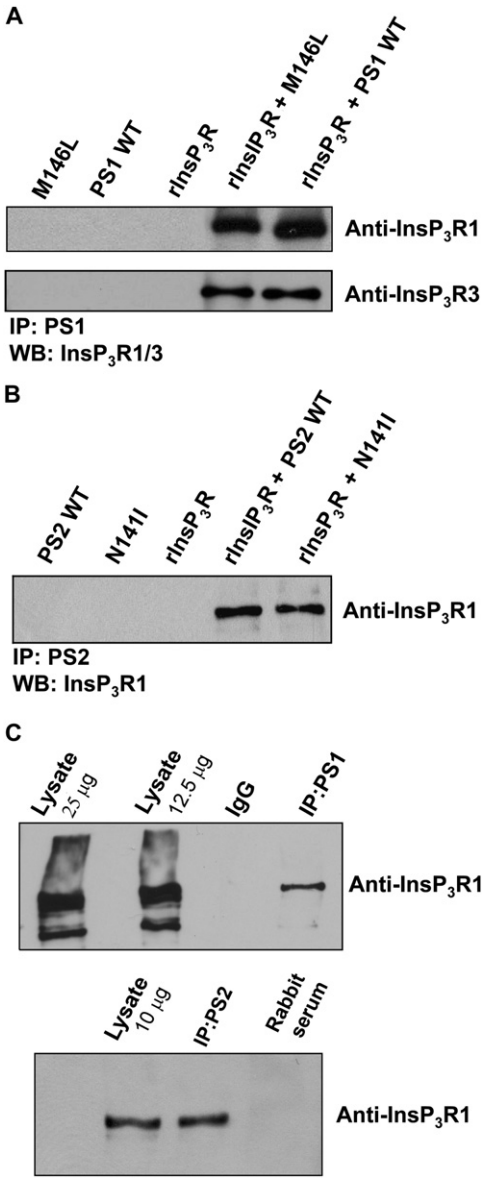

Figure 2. Biochemical Interaction between PS and $InsP_3R$

Western blot of PS1 (A) or PS2 (B) immunoprecipitates from lysates of Sf9 cells coexpressing either PS1-WT or PS1-M146L (A) or PS2-WT or PS2-N141I (B) with rat $InsP_3R$ isoforms 1 or 3; expressed proteins shown at top and probing antibodies shown on right.

(C) Western blots of PS1 (top) and PS2 (bottom) immunoprecipitates from mouse brain lysate. Top: lanes 1 and 2, total input; lane 3, IgG immunoprecipitate control; lane 4, PS1 immunoprecipitate. Bottom: lane 1, total input; lane 2, PS2 immunoprecipitate; lane3, rabbit serum immunoprecipitate control.

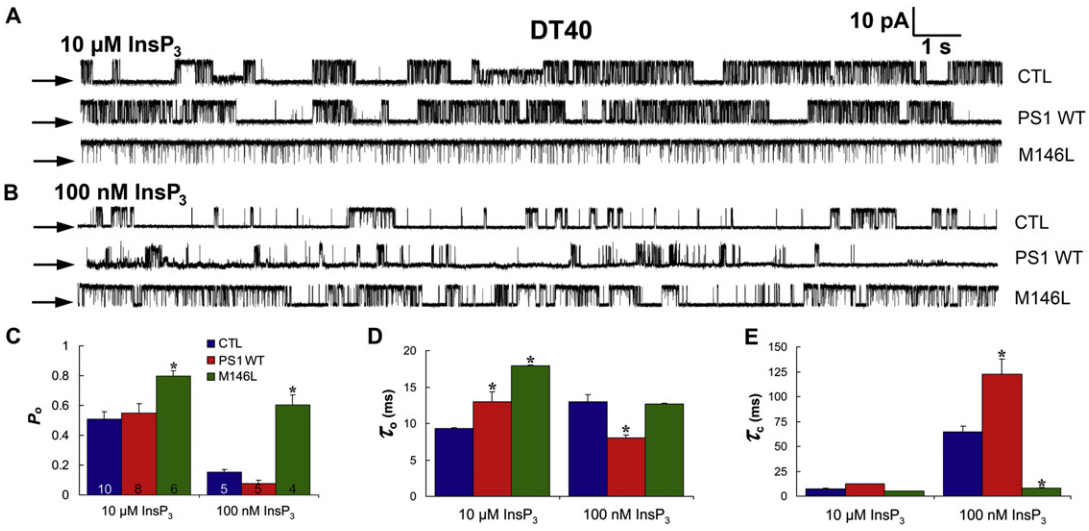

Figure 3. Effects of PS1 Expression on InsP$_3$R Single-Channel Activity in DT40 Cells

Representative InsP$_3$R single-channel current recordings in presence of saturating (10 μM; A) or subsaturating (100 nM; B) InsP$_3$ in DT40 cells stably transfected with PS1 WT or M146L. Pipette [Ca^{2+}] was 1 μM, optimal for channel activity; arrows: zero current level. Summary of effects of PS1 expression on InsP$_3$R P_o (C), mean open time (τ_o) (D), and mean closed time (τ_c) (E). Bars indicate standard error of the mean. Asterisks: $p < 0.01$, unpaired t test. Data presented in Table S2.

The similar behaviors of InsP$_3$R gating from different species in different cell systems in response to expression of FAD mutant and WT PS1 strongly suggests that this is a fundamental channel regulatory mechanism.

Modulation of InsP$_3$R Channel Activity by PS2

Altered [Ca^{2+}]$_i$ signaling has been observed in cells expressing either FAD mutant PS1 or PS2 (Gandy et al., 2006; LaFerla, 2002; Smith et al., 2005a; Stutzmann, 2005). Like PS1, wild-type PS2 (PS2-WT) and FAD mutant PS2 N141I (PS2-N141I) also localized to the nuclear envelope (Figure S2) and interacted biochemically with the InsP$_3$R (Figures 2B and 2C). With 10 μM InsP$_3$ in the pipette solution, InsP$_3$R channels from PS2-WT-infected cells (Figure S1) had P_o similar to those from mock-infected cells ($p > 0.05$; Figures 4A and 4C; Table S3). In contrast, P_o was elevated ($p < 0.05$) in PS2-N141I expressing cells (P_o = 0.81 ± 0.02; Figure 4C). As observed for PS1-M146L, many channels observed in PS2-N141I nuclei were "locked open" (as in Figure 4A). With subsaturating [InsP$_3$], P_o in patches from PS2-N141I nuclei was elevated by nearly 3-fold compared with P_o observed in nuclei from mock or PS2-WT-expressing cells (Figure 4C). Similar to the effect of PS1-M146L, elevated P_o was caused primarily by marked enhancement of the opening rate and prolongation of the mean open time (Figures 4D and 4E). PS2-WT was without effect on channel P_o (Figures 4B and 4C), but it influenced gating, reflected as increases in the mean closed and open times (Figures 4D and 4E). These effects of WT and FAD mutant PS2 on InsP$_3$R gating are highly similar to those observed for WT and mutant PS1, respectively, strongly suggesting that aberrant modulation of InsP$_3$R channel gating is a general property of FAD mutant PS.

Exaggerated Ca^{2+} Signaling in Mutant PS1-Expressing Cells

To address whether these effects of FAD mutant PS observed at the single-channel level account for altered [Ca^{2+}]$_i$ signaling in AD cells, InsP$_3$R-mediated Ca^{2+} signals were recorded in the DT40 cell lines that were used for the single-channel studies and that had comparable levels of InsP$_3$R expression (Figure S3). Physiological InsP$_3$R-mediated Ca^{2+} signals were elicited by crosslinking the B cell receptor (BCR). A high concentration of anti-IgM (5 μg/ml) triggered a rapid increase in [Ca^{2+}]$_i$ in control cells (Figure 5A) due to InsP$_3$-mediated Ca^{2+} release from intracellular stores (Sugawara et al., 1997). In PS1-WT-expressing cells, the magnitude and kinetics were similar to those observed in control cells. In contrast, exaggerated [Ca^{2+}]$_i$ responses were observed in PS1-M146L-expressing cells (Figure 5A), with the peak response over 1.5-fold higher than in control or PS1-WT-expressing cells (Figure 5B). Thus, the DT40 cell system recapitulates the exaggerated [Ca^{2+}]$_i$ responses observed in peripheral cells from FAD patients and neuronal and nonneuronal animal and model cells expressing FAD mutant PS. In response to a low anti-IgM concentration (0.05 μg/ml) expected to generate less InsP$_3$, repetitive [Ca^{2+}]$_i$ oscillations were triggered in 52% ± 5% of control cells (Figures 5C and 5D), due to periodic Ca^{2+} release through the InsP$_3$R (White et al., 2005) after a long lag period (Figure 5F) as [InsP$_3$] increased to levels sufficient for channel stimulation. In cells expressing PS1-M146L, the peak amplitude of the oscillations was similar to those observed in control and PS1-WT-expressing cells (Figure S4), whereas both the oscillation frequency and number of responding cells were increased, and the latency between application of agonist and the first [Ca^{2+}]$_i$ response was decreased (Figures 5C–5F). Of note, the latency was nearly abolished in

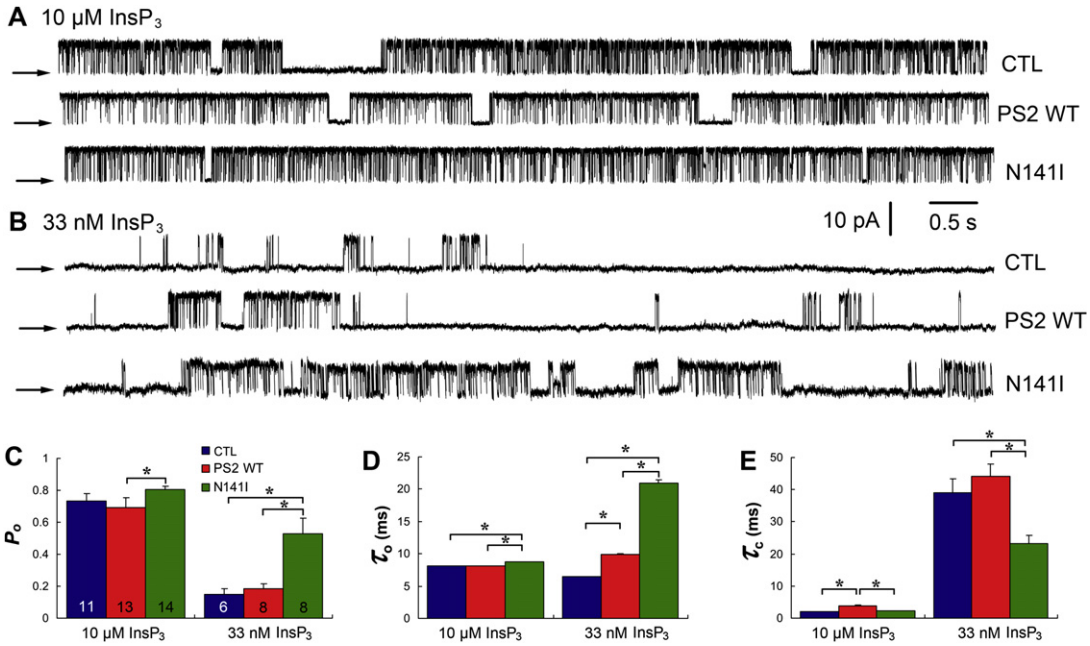

Figure 4. Effect of PS2 on InsP$_3$R Single-Channel Activity in Sf9 Cells

(A and B) Representative current recordings in isolated nuclei from Sf9 cells infected with PS2 WT or N141I baculovirus in the presence of saturating (10 μM; A) or subsaturating (33 nM; B) InsP$_3$. Pipette [Ca^{2+}] was 1 μM; arrows: zero current level. Summary of effects of PS2 expression on InsP$_3$R P_o (C), channel mean open time (τ_o) (D), and channel mean closed time (τ_c) (E). Bars indicate standard error of the mean. Asterisks: $p < 0.01$, unpaired t test. Data presented in Table S3.

a significant subset (~30%) of cells expressing PS1-M146L (Figures 5C and 5F). This response is highly reminiscent of that of control cells to saturating concentrations of BCR antibody (Figure 5A) and was never observed in control or PS1-WT-expressing cells. Increased number of oscillating cells, enhanced oscillation frequency and diminished latencies are all consistent with a heightened InsP$_3$ sensitivity of InsP$_3$R-mediated Ca^{2+} release in the FAD mutant PS1-expressing cells. Interestingly, the number of responding cells was increased and the latency was shortened in the PS1-WT-expressing cells (Figures 5D and 5E), although to a lesser extent than the more exaggerated responses observed in cells expressing FAD mutant PS1.

Spontaneous InsP$_3$R-dependent [Ca^{2+}]$_i$ oscillations were observed in ~6% of control cells perfused with Hank's balanced salt solution without stimulation (Figures 5G and 5H), as observed previously (White et al., 2005). Expression of PS1-WT approximately doubled the percentage of cells displaying this behavior (Figure 5H). In contrast, a 4-fold higher percentage, ~25%, of the PS1-M146L-expressing cells exhibited spontaneous [Ca^{2+}]$_i$ oscillations (Figure 5H). Furthermore, the oscillation frequency in these cells was also enhanced (Figure 5I). In a subset of the mutant PS1-expressing cells (~4%), spontaneous exaggerated [Ca^{2+}]$_i$ transients were observed that were never seen in control and PS1-WT-expressing cells (Figure 5G).

These results are congruent with those obtained in the single-channel studies. In both sets of experiments, exaggerated responses to InsP$_3$, particularly under conditions of low [InsP$_3$], were observed in the context of FAD mutant PS1 expression, with PS1-WT expression also having effects, but much less exaggerated. The congruence of two very different sets of data suggests that the observed exaggerated [Ca^{2+}]$_i$ responses are due to the observed exaggerated InsP$_3$R single-channel responses.

Exaggerated Ca^{2+} Signaling in Mutant PS1-Expressing Cells is Due to Altered InsP$_3$R Gating

Exaggerated [Ca^{2+}]$_i$ responses have been a consistent observation in cells expressing mutant PS proteins (LaFerla, 2002; Smith et al., 2005a; Stutzmann, 2005; Yoo et al., 2000), but it has been suggested that they are caused by enhanced expression of release channels (Chan et al., 2000; Kasri et al., 2006; Schneider et al., 2001; Smith et al., 2005b; Stutzmann et al., 2006) or overfilling of ER Ca^{2+} stores (Leissring et al., 2000; Leissring et al., 2001; Schneider et al., 2001; Tu et al., 2006). We therefore examined whether either factor contributed to the exaggerated [Ca^{2+}]$_i$ responses observed here in DT40 cells. All three cell lines expressed approximately equal levels of the types 1 and 3 InsP$_3$R (Figure S3). Thus, the exaggerated responses cannot be accounted for by altered InsP$_3$R expression in our studies. To investigate the filling state of intracellular Ca^{2+} stores, we evaluated [Ca^{2+}]$_i$ responses to the Ca^{2+} ionophore ionomycin or the SERCA inhibitor thapsigargin applied in the absence of extracellular Ca^{2+} so that the observed [Ca^{2+}]$_i$ responses were due entirely to Ca^{2+} derived from intracellular compartments. Ionomycin (5 μM) triggered a rapid release of Ca^{2+} that was diminished in the PS1-M146L- but not PS1-WT-expressing cells (Figure S5). Similarly, Ca^{2+} released in response to thapsigargin (1 μM) was also significantly reduced in the mutant

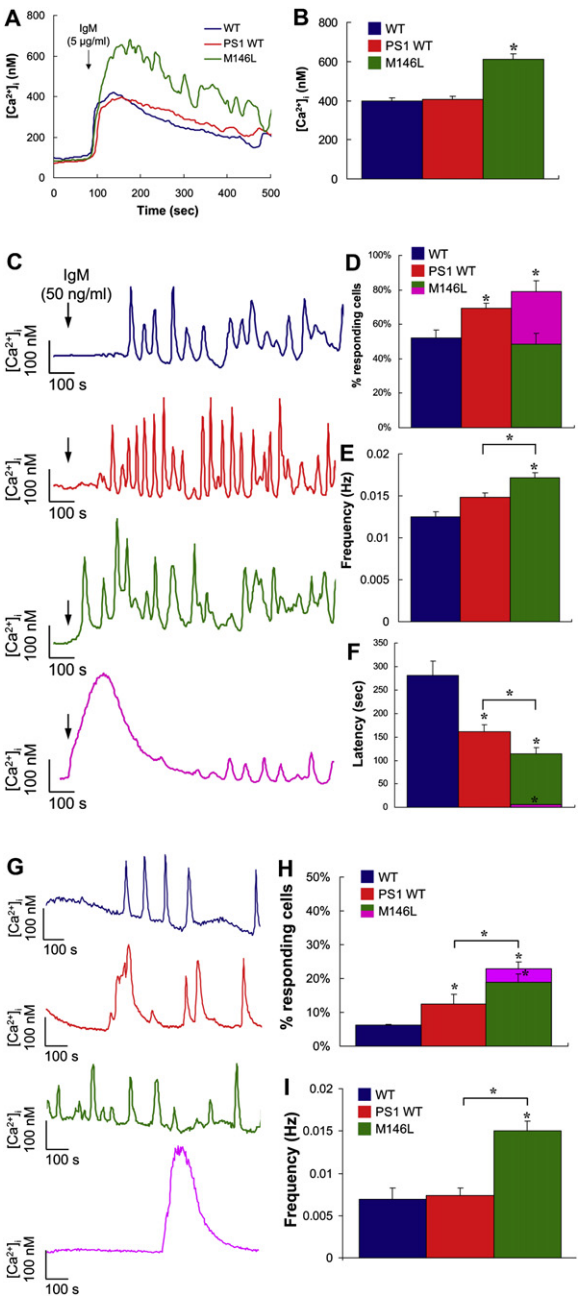

Figure 5. Exaggerated $[Ca^{2+}]_i$ Signaling in Mutant PS-Expressing DT40 Cells

(A and B) Responses to strong stimulation by BCR antibody of DT40 cell $[Ca^{2+}]_i$. (A) Representative single-cell responses to 5 μg/ml anti-IgM (added at arrow) in untransfected (blue) and PS1-WT (red) and PS1-M146L (green) stably-transfected DT40 cells. (B) Summary of peak $[Ca^{2+}]_i$ responses triggered by 5 μg/ml anti-IgM (n = 90). Asterisk: $p < 0.01$ compared with WT and PS1-WT.

(C–F) Responses to weak stimulation by BCR antibody of DT40 cell $[Ca^{2+}]_i$. (C) Representative single cell $[Ca^{2+}]_i$ responses to 50 ng/ml anti-IgM (IgM; added at arrow) stimulation of BCR in control (blue), PS1-WT (red) and PS1-M146L (green and pink) stably transfected DT40 cells. (D) Summary of percentage of cells responding to 50 ng/ml anti-IgM (n = 90). Approximately thirty percent (purple) of PS1-M146L-expressing cells exhibited a different, exaggerated $[Ca^{2+}]_i$ response. (E) $[Ca^{2+}]_i$ oscillation frequency triggered by anti-IgM in WT DT40, PS1-WT-expressing, and PS1-M146L-expressing cells. (F) Summary of latencies to first response in WT DT40, PS1-WT-expressing, and PS1-M146L-expressing cells. The 30% of PS1-M146L-expressing cells that exhibited the exaggerated response had nearly no latency (purple).

(G–I) Spontaneous $[Ca^{2+}]_i$ oscillations in PS1-expressing DT40 cells. (G) Representative spontaneous single-cell $[Ca^{2+}]_i$ oscillations in control (blue) and PS1-WT (red) and PS1-M146L (green and purple) stably transfected DT40 cells. Some PS1-M146L-expressing cells (~4%, purple) displayed a distinct, exaggerated spontaneous $[Ca^{2+}]_i$ signal (bottom). (H) Percentage of cells displaying spontaneous $[Ca^{2+}]_i$ oscillations (n = 90). (I) Spontaneous $[Ca^{2+}]_i$ oscillation frequency observed in WT DT40 cells and PS1-WT- and PS1-M146L-expressing DT40 cells.

Asterisks: $p < 0.01$ compared with WT DT40 cells. Asterisks with bars: $p < 0.01$ PS1-WT versus PS1-M146L. Bars indicate standard error of the mean.

PS1-expressing cells and, to a lesser extent, in the PS1-WT-expressing cells (Figure S5). These results suggest that the Ca^{2+} stores are not overloaded in mutant PS1-expressing cells and may in fact even be reduced. To examine the filling state of the ER Ca^{2+} stores more directly, ER $[Ca^{2+}]$ was measured with the low-affinity fluorescence indicator Mag-Fura-2 (Laude et al., 2005). Addition of MgATP to a solution bathing permeabilized cells with Ca^{2+} stores depleted (not shown) enhanced the fluorescence ratio as a consequence of SERCA-mediated loading of intracellular stores with Ca^{2+} (Figure 6). At steady state, the stores in the FAD PS1-expressing cells were loaded less fully than in control or PS1-WT-expressing cells (Figure 6A; $p < 0.01$), confirming that the Ca^{2+} stores are not overloaded in the mutant PS1-expressing cells. In contrast, when loading was performed in the presence of the $InsP_3R$ inhibitor heparin, the steady-state level of ER Ca^{2+} was similar in all the cell lines (Figure 6B). Thus, the exaggerated $[Ca^{2+}]_i$ responses observed in mutant PS1-expressing DT40 cells (Figure 5) cannot be accounted for by overfilling of ER Ca^{2+} stores. Rather, a reduced ER Ca^{2+} was observed in the FAD-PS1 expressing cells that appeared to be due an activated heparin-sensitive Ca^{2+} leak through the $InsP_3R$. This was more directly examined by use of a different protocol, in which the Ca^{2+} leak permeability of the ER membrane was measured following the addition of thapsigargin to cells with ER stores filled with Ca^{2+} to equivalent levels. The Ca^{2+} leak rate was similar in control and PS1-WT cells, whereas it was greater in the FAD mutant PS1-expressing cells (Figures 6C and 6D). This enhanced Ca^{2+} leak observed in the PS1-M146L cells was eliminated by addition of heparin (Figures 6E and 6F), suggesting that it was mediated by the $InsP_3R$. To test this rigorously, we generated stable PS1-expressing DT40 cells with genetic disruption of all three $InsP_3R$ genes (Sugawara et al., 1997). In the absence of $InsP_3R$ expression (Figure S3), both anti-IgM-induced and spontaneous $[Ca^{2+}]_i$ signals were absent (not shown). Notably, the sizes of the intracellular Ca^{2+} stores in the PS1-M146L- or PS1-WT-expressing cells were similar in the $InsP_3R$-deficient cells (Figure 6G). Importantly, the enhanced PS1-M146L induced ER Ca^{2+} leak rate was absent in the $InsP_3R$-deficient cells (Figure 6H). These results demonstrate that exaggerated Ca^{2+} signaling, reduced Ca^{2+} store size, and enhanced ER Ca^{2+} leak permeability are specific properties of PS1-M146L-expressing cells and, furthermore, that these features are completely dependent on the $InsP_3R$. Together, these results strongly

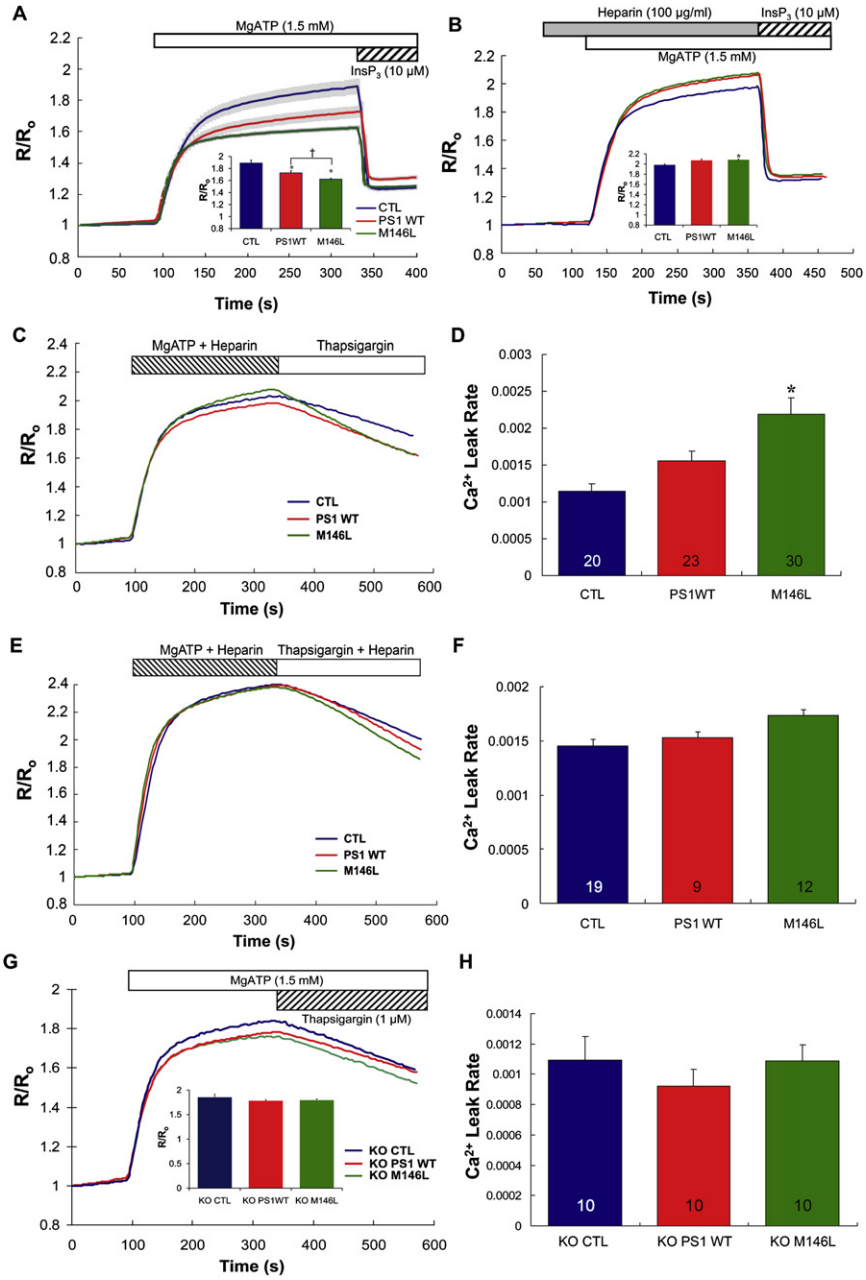

Figure 6. The Amount of Ca^{2+} in the ER Store Is Not Increased by PS1-M146L Expression, Due to FAD Mutant PS1- and $InsP_3R$-Dependent Enhanced Ca^{2+} Leak Permeability of the ER Membrane

(A) ER [Ca^{2+}] expressed as Mag-Fura-2 ratio normalized to ratio at t = 0 before and then during filling upon addition of MgATP (1.5 mM) and subsequent emptying by addition of $InsP_3$ (10 μM) in control (blue) and PS1-WT (red) and PS1-M146L (green) stable DT40 cells. Insert: Steady-state ER [Ca^{2+}] in presence of MgATP. Asterisks: $p < 0.01$ compared with control cells. Cross: $p < 0.01$ compared with PS1-WT.

(B) Similar experiment with ER Ca^{2+} loading performed in presence of heparin (100 μg/ml). Asterisk: $p < 0.01$ and < 0.05 compared with control and PS1-WT cells, respectively.

(C) ER [Ca^{2+}] during filling upon addition of MgATP (1.5 mM) in presence of heparin (100 μg/ml) and then after removal of MgATP and addition of thapsigargin (1 μM), in control (blue), and PS1-WT (red) and PS1-M146L (green) stable DT40 cells.

(D) Summary of ER Ca^{2+} leak rate, calculated as initial rate of decline of the Mag-Fura-2 ratio. Asterisk: enhanced leak observed in M146L-expressing cells compared with control and PS1-WT ($p < 0.01$).

(E) Similar experiments as in (D), except that heparin (100 μg/ml) was present during measurements of the Ca^{2+} leak rate.

(F) Summary of ER Ca^{2+} leak rate in presence of heparin.

(G) Similar experiment as in (D) performed in cells lacking $InsP_3R$ expression (KO). Insert: steady-state ER [Ca^{2+}] after MgATP-induced loading.

(H) Summary of ER Ca^{2+} leak rate in PS1 expressing $InsP_3R$ KO cells.

Bars indicate standard error of the mean.

suggest that mutant PS1-M146L diminishes the size of the ER Ca^{2+} store by a mechanism that involves its enhancement of $InsP_3R$ channel activity, a process that disrupts the normal Ca^{2+} pump/leak balance in favor of enhanced leak mediated by $InsP_3$-dependent $InsP_3R$-mediated Ca^{2+} permeability. We conclude, therefore, that the observed altered $InsP_3R$ single-channel activity most likely accounts for the altered $[Ca^{2+}]_i$ signals observed.

FAD Mutant PS1 Enhances $InsP_3R$-Mediated ER Ca^{2+} Permeability in Brain Neurons

Whereas FAD mutant PS associated exaggerated Ca^{2+} signaling has been observed in many cell types, AD pathophysiology is manifested primarily in brain neurons. To determine if FAD PS1 expression was associated with altered $InsP_3R$-mediated Ca^{2+} release in brain neurons, cortical neurons were isolated from E15–E16 mouse brains, and the Ca^{2+} permeability properties of the ER membranes were measured as above (Figure 7A). The steady-state level of Ca^{2+} accumulated in the ER lumen was not different between control cells and neurons expressing either WT or M146L-PS1 (Figure 7B). The Ca^{2+} leak permeability measured upon addition of thapsigargin was somewhat higher in PS1-M146L expressing neurons than in those expressing PS1-WT ($p < 0.05$), although it was not different compared with control cells (Figure 7C). In a separate set of experiments (Figure 7D), 33 nM $InsP_3$ failed to elicit Ca^{2+} release in control or PS1-WT cells, whereas it simulated Ca^{2+} release from the ER of PS1-M146L cells (Figure 7E), with an initial rate that was comparable to that achieved by addition of saturating (10 μM) $InsP_3$ to the control cells (Figure 7F). Thus, as in the non-neuronal cells examined, FAD mutant PS1 specifically sensitizes $InsP_3R$-mediated Ca^{2+} release in brain cortical neurons.

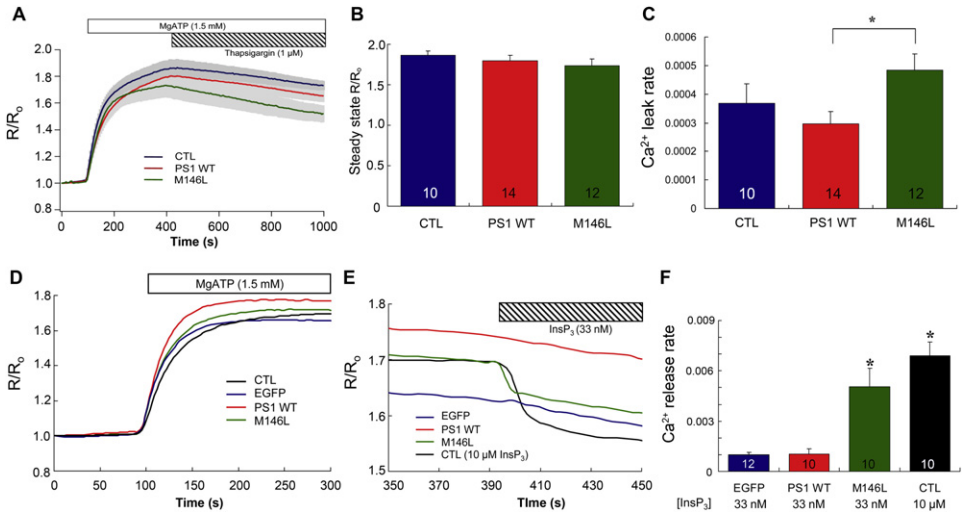

Figure 7. FAD Mutant PS1 Enhances $InsP_3R$-Mediated ER Ca^{2+} Permeability in Brain Neurons

(A) ER $[Ca^{2+}]$, expressed as Mag-Fura-2 ratio normalized to ratio at t = 0, before and then during filling upon addition of MgATP (1.5 mM), and subsequent exposure to 1 μM thapsigargin in control (blue) and PS1-WT (red)- and PS1-M146L (green)-transfected mouse cortical neurons.

(B) Summary of steady-state ER $[Ca^{2+}]$ following MgATP-induced loading in (A).

(C) Summary of Ca^{2+} leak rate measured in presence of thapsigargin in (A). Asterisk: p = 0.01.

(D) ER $[Ca^{2+}]$ during filling upon addition of MgATP (1.5 mM) in control (black) and EGFP (blue)-, PS1-WT (red)-, and PS1-M146L (green)-transfected mouse cortical neurons.

(E) Response of ER $[Ca^{2+}]$ to 33 nM $InsP_3$ in cells from (D) and in control cells in response to 10 μM $InsP_3$ (black trace).

(F) Summary of initial Ca^{2+} release rate, expressed as Mag-Fura-2 ratio, from (E).

Asterisks: $p < 0.01$ compared with control and PS1-WT. Bars indicate standard error of the mean.

Functional Consequences of $InsP_3R$-PS1 Interaction—APP Processing

Identification of a molecular mechanism that links FAD mutant PS to altered $[Ca^{2+}]_i$ signaling provides an opportunity for insights into relationships between pathological features of AD and altered $[Ca^{2+}]_i$ signaling. PS1 is the core subunit of the γ-secretase that enzymatically cleaves APP into amyloid peptides, including $Aβ_{40}$ and $Aβ_{42}$ (Edbauer et al., 2003). FAD PS mutations alter secretase function by either modifying its sequence specificity or absolute activity, such that the relative proportion or amount of $Aβ_{42}$ produced is increased (Citron et al., 1997; Scheuner et al., 1996). To determine the relevance of the functional interaction of PS1 and $InsP_3R$ for APP processing, we engineered DT40 cells to stably express APP harboring Swedish mutations (APP_{SWE}) that enhance production of Aβ species (Scheuner et al., 1996), together with either PS1-WT or PS1-M146L (Figure 8A). PS1-M146L specifically enhanced $Aβ_{40}$ and $Aβ_{42}$ by ~2- and ~3-fold, respectively, compared with control cells. This result is consistent with observations in other cell types (Citron et al., 1997), validating again the use of this model system. Of note, the $Aβ_{42}/Aβ_{40}$ ratio was enhanced in the FAD mutant PS1-expressing cells (Figure 8), as observed in AD patients. To determine the role of the $InsP_3R$ in PS1-dependent APP processing, APP and PS1-expxressing cells were generated in the $InsP_3R$-KO background, and APP processing was similarly evaluated. Remarkably, the mutant PS1 enhancement of Aβ secretion observed in the $InsP_3R$-expressing cells was abolished. Furthermore, the absolute levels of Aβ peptides detected were strongly reduced in all control and PS1-expressing $InsP_3R$-KO lines (Figure 8B). These results indicate that altered APP processing by mutant PS1-M146L PS1 has a strong dependence on the $InsP_3R$.

DISCUSSION

The underlying pathogenic mechanisms of Alzheimer's disease remain obscure. In this study, we considered that dysregulated $[Ca^{2+}]_i$ signaling is a proximal mechanism in AD. We used non-neuronal model cell systems because they provided unique advantages for deciphering the molecular mechanisms involved and confirmed the major results in primary brain neurons. Both the $InsP_3R$ (Foskett et al., 2007) as well as presenilins (Hebert et al., 2004) are widely distributed throughout all tissues investigated, with the highest levels of PS expression outside the brain (Hebert et al., 2004), and similar Ca^{2+} signaling abnormalities have been observed in several peripheral and neuronal cell types that express mutant PS (LaFerla, 2002; Smith et al., 2005a; Stutzmann, 2005). We have demonstrated that FAD mutant presenilins interact biochemically and functionally with the $InsP_3R$ Ca^{2+} release channel and exert profound stimulatory effects on its gating activity that result in exaggerated Ca^{2+} signaling in intact cells, including brain neurons. Our results indicate that this functional interaction has physiological implications that may be relevant in AD, including APP processing.

Presenilins Regulate $InsP_3R$ Ca^{2+} Release Channel Gating

We observed that expression of two FAD mutant PS (PS1-M146L and PS2-N141I) each had strong and similar effects on

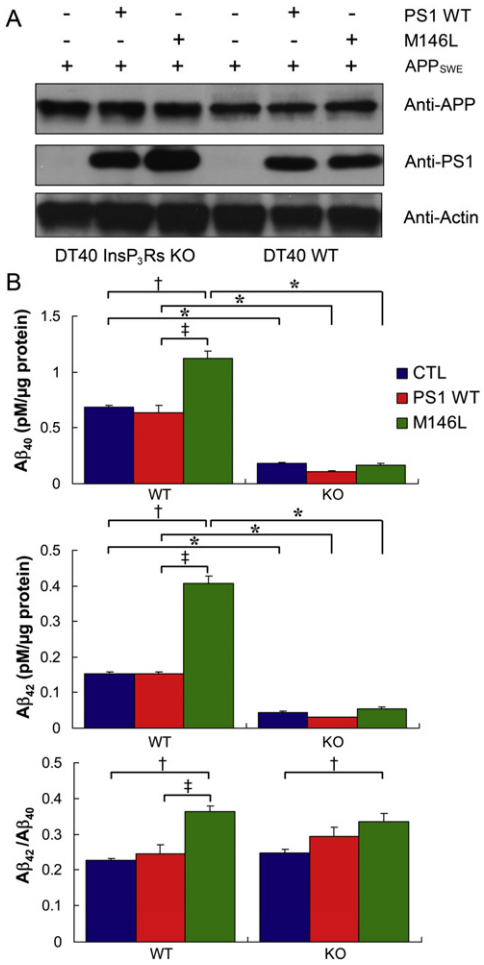

Figure 8. APP Processing Is Dependent on InsP$_3$R

(A) Stable expression of PS1-WT and PS1-M146L proteins in wild-type (WT) and InsP$_3$R-deficient (KO) DT40 cell lines that stably expressed APP$_{SWE}$. Actin probed as loading control.

(B) ELISA measurements of Aβ$_{40}$ (top), Aβ$_{42}$ (middle), and Aβ$_{42}$/Aβ$_{40}$ ratio (bottom) secreted over 48 hr by InsP$_3$R-expressing wild-type (WT; left) or InsP$_3$R-deficient (KO DT40 cells; right) DT40 cells stably expressing APP$_{SWE}$ alone (blue) or APP$_{SWE}$ with PS1-WT (red) or PS1-M146L (green).

Bars indicate standard error of the mean. Asterisks: $p < 0.01$ compared with control WT cells. Cross: $p < 0.01$ compared with control WT cells; double cross: $p < 0.01$ compared with PS1-WT cells.

the gating of single InsP$_3$R Ca^{2+} release channels. We attempted to ensure equal levels of expression of InsP$_3$R and the different PS proteins among the different groups of cells, but this could not be achieved perfectly. Nevertheless, because very similar results were obtained in two very distinct cell systems, Sf9 and DT40 cells, this was likely not a significant confounding variable. In both systems, mutant PS expression caused the InsP$_3$R channel to gate as actively in low submaximal [InsP$_3$] as it normally does in saturating [InsP$_3$]. Elevated P_o in low [InsP$_3$] by FAD mutant PS was caused primarily by a substantial increase of channel opening rate, the major mechanism whereby InsP$_3$ activates the channel (Foskett et al., 2007), indicating that mutant PS enhances InsP$_3$R gating by sensitizing it to low [InsP$_3$]. This mechanism is likely an allosteric one mediated by interaction of PS with the InsP$_3$R that is preserved in isolated nuclei. Both membrane proteins localized to the nuclear envelope and mutant- as well as WT-PS coimmunoprecipitated to the same extent with mammalian InsP$_3$R, suggesting that PS mutations do not strongly affect the biochemical interaction. Although WT PS1 or PS2 did not affect channel P_o, small effects on InsP$_3$R channel gating were nevertheless observed. It has been debated whether FAD PS mutations are gain or loss of function (Shen and Kelleher, 2007). Here, we show an apparent gain in InsP$_3$R function by FAD mutant PS expression. However, channel dwell time analyses suggest that WT PS1 and PS2 also influence InsP$_3$R channel gating. It is possible therefore that the gain-of-function phenotype we observe is due to disruption by mutant PS of normal PS-WT regulation of InsP$_3$R channel activity. Future studies of the InsP$_3$R gating behaviors in PS-deficient cells will be informative in this regard.

FAD Mutant PS1-Mediated Enhanced InsP$_3$R Gating Causes Exaggerated [Ca^{2+}]$_i$ Signaling

Analysis of our single-channel data suggests that mutant PS1 and PS2 stimulate InsP$_3$R gating by sensitizing the channel to InsP$_3$. One of the most consistent observations of the effects of FAD PS on Ca^{2+} signaling is potentiation of InsP$_3$-mediated Ca^{2+} release (Smith et al., 2005a; Yoo et al., 2000). Nevertheless, the molecular mechanisms have remained obscure. InsP$_3$-mediated [Ca^{2+}]$_i$ signals in FAD patient fibroblasts were exaggerated in response to low agonist concentrations (Ito et al., 1994), consistent with an enhanced sensitivity to InsP$_3$ in AD. The magnitude and rate of [Ca^{2+}]$_i$ rise in response to photo-release of InsP$_3$ were enhanced by FAD mutant PS in *Xenopus* oocytes (Leissring et al., 1999a, 1999b). Furthermore, Ca^{2+} puffs, low-level Ca^{2+} release events mediated by clusters of InsP$_3$R in response to submaximal [InsP$_3$], were both more frequent and likely to generate [Ca^{2+}]$_i$ waves in the FAD mutant PS-expressing cells (Leissring et al., 2001). In brain slices from PS1-M146V knockin mice, photo-release of InsP$_3$ caused 3-fold greater Ca^{2+} release than in nontransgenic neurons and enhanced the number of neurons responding and those exhibiting strong responses (Stutzmann et al., 2004). By demonstrating that mutant PS sensitizes the InsP$_3$R to InsP$_3$, our new results provide a molecular mechanism that is consistent with these previous observations and can therefore possibly account for them. To test this idea, the relevance of the observed effects of FAD PS1 expression on InsP$_3$R single-channel gating was determined by measuring [Ca^{2+}]$_i$ responses in PS-expressing DT40 cells, the same cells used for the single-channel studies, that had comparable levels of InsP$_3$R expression. Exaggerated Ca^{2+} release responses to both high- as well as low-threshold concentrations of agonist were observed in the cells that expressed the PS1-M146L protein. In a significant proportion of the FAD mutant PS-expressing cells, the [Ca^{2+}]$_i$ responses to low agonist concentrations mimicked the responses of normal cells to a saturating agonist concentration. Furthermore, a high percentage of PS1-M146L-expressing unstimulated cells displayed spontaneous low-level [Ca^{2+}]$_i$ signals in the absence of agonist stimulation. Most importantly, the exaggerated Ca^{2+} responses were mediated specifically by the InsP$_3$R, since they were absent in

$InsP_3R$ knockout cells. All these features are consistent with an enhanced $InsP_3$ sensitivity of the $InsP_3R$ in intact cells expressing FAD mutant PS, even to [$InsP_3$] that may exist in resting, unstimulated cells. The conclusions based on the effects of PS1-M146L expression on $[Ca^{2+}]_i$ signals are therefore in strong agreement with those reached from the single-channel studies. Thus, these results suggest that exaggerated $[Ca^{2+}]_i$ signals in cells can be accounted for by exaggerated $InsP_3R$ gating as a result of its interaction with FAD mutant PS. Importantly, these insights appear to be relevant for brain neurons, since $InsP_3R$-mediated ER Ca^{2+} permeability was enhanced by FAD mutant PS1 expression in mouse brain cortical neurons, enabling Ca^{2+} release to be triggered by low [$InsP_3$] that were without effect in either control cells or cells expressing WT PS1.

It has been suggested that exaggerated Ca^{2+} release in AD cells is due to increased filling of ER Ca^{2+} stores (discussed in LaFerla, 2002; Mattson and Chan, 2003; Stutzmann, 2005). Although this "Ca^{2+} overload" hypothesis has been widely invoked, many studies, including ours here, have observed either no alteration or reduced ER Ca^{2+} stores in FAD PS-expressing cells (Giacomello et al., 2005; Lessard et al., 2005; Zatti et al., 2004, 2006). The absence of elevated ER [Ca^{2+}] suggests that the effects of FAD PS on $InsP_3R$ gating observed here cannot be accounted for by possible effects of elevated luminal [Ca^{2+}] on channel function. Furthermore, we have observed in excised luminal side-out nuclear patches that $InsP_3R$ channel gating is insensitive to bath (luminal) [Ca^{2+}] between 100 nM and 500 μM (data not shown). Ca^{2+} release is affected by many variables, including activities and expression of release channels, amount of ER Ca^{2+}, Ca^{2+} buffering, and more. Enhanced spontaneous Ca^{2+} release activity observed in our PS1-M146L-expressing DT40 cells reduced ER Ca^{2+}, but $[Ca^{2+}]_i$ responses to agonists were nevertheless enhanced because of the strong effect of mutant PS on $InsP_3R$ gating. Thus, exaggerated Ca^{2+} release responses cannot provide unambiguous measurements of the amount of Ca^{2+} in stores. Our results demonstrate that effects of FAD mutant PS1 on both $[Ca^{2+}]_i$ signaling and ER Ca^{2+} content are $InsP_3R$ dependent, with mutant PS1- and PS2-stimulated $InsP_3R$ channels remaining regulated by $InsP_3$. Thus, cell type-specific differences in concentrations of $InsP_3R$ ligands and expression levels can contribute to the magnitude of the effect of mutant PS1 expression on ER Ca^{2+}, which might reconcile discrepant published observations. The enhanced Ca^{2+} release responses observed in PS1-M146L-expressing DT40 cells are highly reminiscent of those in peripheral and neuronal mutant PS-expressing cells in many previous studies. The absence of these responses in $InsP_3R$-knockout cells, together with the identification of a molecular mechanism observed at the single channel level, strongly suggest that mutant PS-mediated enhancement of $InsP_3$ sensitivity of the $InsP_3R$ is a fundamental underlying mechanism that accounts for many observations of dysregulated Ca^{2+} signaling in AD cells and model cell systems.

It has been reported that exaggerated Ca^{2+} responses in cells expressing FAD mutant PS are associated with enhanced expression or activities of ryanodine receptor (RyR) Ca^{2+} release channels (Chan et al., 2000; Smith et al., 2005b; Stutzmann et al., 2006). In AD-transgenic mouse cortical neurons, exaggerated responses to $InsP_3$ were mediated in part by RyR activated by Ca^{2+} released through $InsP_3R$ (Stutzmann et al., 2006), suggesting that exaggerated RyR responses could be a secondary effect. Because Ca^{2+} signaling can influence $InsP_3R$ (Cai et al., 2004; Genazzani et al., 1999) and RyR (P. Nicotera, personal communication) expression, it is possible that mutant PS-mediated enhanced $InsP_3R$ Ca^{2+} signaling drives transcriptional programs, with RyR expression upregulated as a result. Conversely, Aβ exposure increased RyR expression in mouse cortical neurons (Supnet et al., 2006), suggesting that changes in RyR expression may be more downstream compared with a more proximal $InsP_3R$-mediated process described here. Alternately, PS and RyR may functionally interact similar to the PS-$InsP_3R$ interaction. PS2 has been reported to interact with RyR2, the cardiac isoform, and PS2 knockout results in cardiac Ca^{2+} signaling abnormalities (Takeda et al., 2005). In addition, WT and mutant PS1 have been reported to interact with RyR3 (Chan et al., 2000).

It was proposed that reconstituted PS proteins form divalent cation-permeable ion channels in bilayer membranes and that loss of this function in FAD PS enhanced ER Ca^{2+}, resulting in exaggerated Ca^{2+} release responses (Nelson et al., 2007; Tu et al., 2006). In contrast, we did not detect in native ER membranes a cation permeability associated with either WT or FAD mutant PS expression. Furthermore, we found that FAD mutant PS expression either reduced (DT40 cells) or had no effect (cortical neurons) on the amount of Ca^{2+} in the ER. Thus, our experiments failed to discover evidence in support of the hypothesis that PS form ion channels.

Finally, it should be emphasized that the Ca^{2+} signaling abnormalities we observed represent proximal mechanisms distinct from effects of Aβ on Ca^{2+} signaling (Mattson and Guo, 1997). Our studies indicate the presence of a complex involving PS and $InsP_3R$ that results in hyperactivation of the Ca^{2+} release channel in a process that is independent of Aβ.

Enhanced PS-Dependent $InsP_3R$-Mediated Ca^{2+} Signaling Enhances Aβ Processing

Disrupted Ca^{2+} signaling in AD cells has been well documented, but its physiological implications and the roles that these changes play in AD pathogenesis have not been well studied. Altered Ca^{2+} signaling could impinge on synaptic plasticity, membrane excitability, oxidative stress, and APP processing. Identification of the $InsP_3R$ as a molecular mechanism of Ca^{2+} disruption associated with FAD PS now suggests specific hypotheses that can be tested to evaluate the relevance of altered Ca^{2+} signaling through this pathway on disease-associated processes.

Our data suggest that one function of PS proteins may be to regulate the activity of the $InsP_3R$. Is there a relationship between this activity and the activity of PS as secretases? APP processing can be enhanced by elevations of $[Ca^{2+}]_i$ (Buxbaum et al., 1994; Jolly-Tornetta et al., 1998; Querfurth and Selkoe, 1994) and diminished by inhibition of ER Ca^{2+} release (Buxbaum et al., 1994). APP processing was examined in DT40 cells lines engineered to stably express PS1 and APP_{SWE}, exploiting DT40 KO cells as the only cell type available that completely lacks $InsP_3R$ expression. Expression of PS1-M146L caused a nearly 3-fold increase in $Aβ_{42}$ compared with control and

PS1-WT-expressing cells. Consequently, $A\beta_{42}/A\beta_{40}$ increased ~2-fold, recapitulating an important feature of AD (Haass and Selkoe, 2007). Importantly, APP processing appeared to be strongly dependent on the $InsP_3R$, since production of $A\beta_{40}$ and $A\beta_{42}$ were substantially lower in $InsP_3R$-deficient lines. Furthermore, the PS1-M146L enhancement of $A\beta_{42}$ and $A\beta_{42}/A\beta_{40}$ were eliminated in the $InsP_3R$-KO cells. These results suggest that the γ-secretase activity of WT and FAD mutant PS may be regulated by either Ca^{2+} released through the $InsP_3R$, or their biochemical interaction with the channel. Our studies suggest that $InsP_3R$ activity affects APP processing, but pharmacological inhibition of γ-secretase is without effect on $InsP_3R$-mediated Ca^{2+} signaling (Oh and Turner, 2006). Thus, the γ-secretase activity of PS is likely not involved in this mechanism by which mutant PS regulates $InsP_3R$ channel gating.

The dependence of Aβ production on $InsP_3R$ expression observed here suggests that mutant PS-mediated exaggerated Ca^{2+} signaling could be a proximal mechanism in AD. Brain Aβ production is driven by neuronal activity (Cirrito et al., 2005; Kamenetz et al., 2003), suggesting that activity and metabolic patterns may contribute to Aβ production and amyloid deposition (Buckner et al., 2005). As-yet-unspecified activity- or metabolism-dependent mechanisms may cause preferential accumulation of amyloid that, over many years, may participate in AD pathology (Buckner et al., 2005). Because of a central role of Ca^{2+} in regulating both neuronal excitability (Verkhratsky, 2005) and cell metabolism (Balaban, 2002; McCormack et al., 1990), active brain regions are likely sites of higher Ca^{2+} signaling activity. Mutant PS-mediated exaggerated Ca^{2+} release activity of the $InsP_3R$ may therefore provide a mechanism for preferential accumulation of amyloid. Other mechanisms that do not involve either PS or $InsP_3R$, but that similarly cause chronic low-level exaggerated Ca^{2+} signaling might also be expected to result in AD pathology. Although speculative, such mechanisms could possibly be involved in sporadic forms of AD.

In summary, our results indicate that PS interact with the $InsP_3R$ Ca^{2+} release channel and modulate its gating activity. FAD mutant PS1 and PS2 exert stimulatory effects on $InsP_3R$ channel activity that result in perturbed cellular Ca^{2+} signaling. These data provide molecular insights into the mechanisms of enhanced $InsP_3$-mediated Ca^{2+} signals observed in cells that express FAD mutant presenilins, including those from AD patients. Enhanced Ca^{2+} release from the ER as a result of this interaction has physiological implications that may be relevant in AD, including enhanced APP processing. These observations may provide unique molecular insights into the "Ca^{2+} dysregulation hypothesis" of AD pathogenesis and suggest novel targets for therapeutic intervention.

EXPERIMENTAL PROCEDURES

Recombinant Baculovirus Constructs and Sf9 Cell Infection

Spodoptera frugiperda cells (Sf9, BD Biosciences) were maintained as described (Ionescu et al., 2006). Human PS baculovirus constructs (PS1-WT, PS1-M146L, PS2-WT, and PS2-N141I) were subcloned into pFastBac1; baculoviruses were generated using the Bac-to-Bac system (Invitrogen). Expression was confirmed by western blotting with anti-PS1 (monoclonal MAB5232, polyclonal MAB1563, Chemicon International, Inc.) and -PS2 (EMD Chemicals Inc.) antibodies. Localization of PS in Sf9 cells was confirmed by immunocytochemistry with anti-PS1 or -PS2 antibodies. Sf9 nuclei were counterstained with TOTO-3 nuclear dye (Molecular Probes).

Cell Culture and Transfection

DT40 cells were maintained as described (White et al., 2005). Human wild-type (WT) *PS1* and *M146L* cDNAs were subcloned into pIRES2-EGFP (Clontech). Cells were transfected using a Nucleofector Device (Amaxa). To select stable polyclonal lines, transfected cells were cultured for 2 weeks in 2 mg ml^{-1} Geneticin (Invitrogen). PS expression was confirmed by western blot. Human APP harboring Swedish mutations (APP_{SWE}) was introduced into PS1-expressing DT 40 lines by retrovirus infection. *APP_{SWE}* cDNA was subcloned into pΔMX-IRES-dsRED retrovirus vector. APP_{SWE} retrovirus was generated using Retro-X system (Clontech). Expression of APP_{SWE} was confirmed by western blotting using a polyclonal anti-APP antibody. Primary cortical neurons were prepared from embryonic day 15 (E15–16) C57BL/6J mice, as described (Meberg and Miller, 2003). Transfections were performed on 7- to 14-day-old cultures with pIRES2-EGFP-PS1WT, pIRES2-EGFP-M146L, or pIRES2-EGFP empty vector by n-Fect reagent (Neuromics). Experiments performed 48 hr after transfection.

Electrophysiology

Preparation of isolated nuclei from Sf9 or DT40 cells was as described (White et al., 2005). Nuclei were studied in standard bath solution: 140 mM KCl, 10 mM HEPES, and 0.5 mM BAPTA (free $[Ca^{2+}]$ = 300 nM) (pH 7.3). The pipette solution contained 140 mM KCl, 0.5 mM ATP, 10 mM HEPES, 1 μM free Ca^{2+} (pH 7.3). Free $[Ca^{2+}]$ in all solutions was adjusted, as described (Mak et al., 1998). Data were acquired at room temperature and analyzed as described (Ionescu et al., 2006).

Single-Cell Ca^{2+} Imaging

$[Ca^{2+}]_i$ was measured in Fura-2-loaded DT40 cells as described (White et al., 2005). ER Ca^{2+} content was estimated from changes in $[Ca^{2+}]_i$ in response to thapsigargin or ionomycin, as described (White et al., 2005), or with the low-affinity Ca^{2+} indicator Mag-Fura-2 (Invitrogen) following procedures similar to those described in Laude et al. (2005) modified for single-cell imaging. Following loading of cells on coverslips with Mag-Fura-2 (10 μM for 60 min), the plasma membranes were permeabilized by exposure to 10 μg/ml digitonin for 2 min in a medium that contained 220 nM Ca^{2+} and lacked MgATP. Following 30 min of continuous perfusion with the MgATP-free bath to wash out the digitonin, cells were alternately illuminated with 340/380 nm light and fluorescence intensity at 510 nm was collected with a Perkin Elmer Ultraview imaging system. Changes in $[Ca^{2+}]_{ER}$ are presented as changes in fluorescence ratio (R/R_0). R_0 was verified to reflect the ratio for Ca^{2+} depleted stores by using ionomycin (1 μM), as described (Laude et al., 2005). Ca^{2+} leak rates expressed as $\Delta(R/R_0)$ s^{-1}.

Amyloid Beta ($A\beta_{40}$ and $A\beta_{42}$) Determinations

Aβ levels in culture media were measured by sandwich ELISA (Suzuki et al., 1994). Briefly, plates were coated with Aβ N-terminal antibody Ban50 prior to application of cell media. The concentration of Aβ was determined using horseradish peroxidase (HRP)-conjugated BA27 or BC05 antibodies to detect $A\beta_{40}$ or $A\beta_{42}$, respectively. $A\beta_{40}$ or $A\beta_{42}$ levels were normalized to total protein concentration. Standard curves, constructed from serial dilutions of synthetic $A\beta_{40}$ or $A\beta_{42}$, were generated in each experiment.

Analysis and Statistics

Data were summarized as the mean ± SEM, and statistical significance of differences between means was assessed using unpaired t tests or analysis of variance (ANOVA) for repeated-measures at the 95% level ($p < 0.05$).

SUPPLEMENTAL DATA

The Supplemental Data for this article can be found online at http://www.neuron.org/cgi/content/full/58/6/871/DC1/.

ACKNOWLEDGMENTS

We thank Ikuo Hayashi for recombinant baculoviruses and Eric Swanson for help with neuron isolation. This work was supported by NIH GM56328 and MH059937 to J.K.F. and a Pilot Project from the Alzheimer's Disease Core Center at the University of Pennsylvania AG 10124.

Received: August 31, 2007
Revised: February 5, 2008
Accepted: April 16, 2008
Published: June 25, 2008

REFERENCES

Balaban, R.S. (2002). Cardiac energy metabolism homeostasis: role of cytosolic calcium. J. Mol. Cell. Cardiol. *34*, 1259–1271.

Barrow, P.A., Empson, R.M., Gladwell, S.J., Anderson, C.M., Killick, R., Yu, X., Jefferys, J.G., and Duff, K. (2000). Functional phenotype in transgenic mice expressing mutant human presenilin-1. Neurobiol. Dis. *7*, 119–126.

Berridge, M.J., Lipp, P., and Bootman, M.D. (2000). The versatility and universality of calcium signalling. Nat. Rev. Mol. Cell Biol. *1*, 11–21.

Blennow, K., de Leon, M.J., and Zetterberg, H. (2006). Alzheimer's disease. Lancet *368*, 387–403.

Buckner, R.L., Snyder, A.Z., Shannon, B.J., LaRossa, G., Sachs, R., Fotenos, A.F., Sheline, Y.I., Klunk, W.E., Mathis, C.A., Morris, J.C., and Mintun, M.A. (2005). Molecular, structural, and functional characterization of Alzheimer's disease: evidence for a relationship between default activity, amyloid, and memory. J. Neurosci. *25*, 7709–7717.

Buxbaum, J.D., Ruefli, A.A., Parker, C.A., Cypess, A.M., and Greengard, P. (1994). Calcium regulates processing of the Alzheimer amyloid protein precursor in a protein kinase C-independent manner. Proc. Natl. Acad. Sci. USA *91*, 4489–4493.

Cai, W., Hisatsune, C., Nakamura, K., Nakamura, T., Inoue, T., and Mikoshiba, K. (2004). Activity-dependent expression of inositol 1,4,5-trisphosphate receptor type 1 in hippocampal neurons. J. Biol. Chem. *279*, 23691–23698.

Cedazo-Minguez, A., Popescu, B.O., Ankarcrona, M., Nishimura, T., and Cowburn, R.F. (2002). The presenilin 1 deltaE9 mutation gives enhanced basal phospholipase C activity and a resultant increase in intracellular calcium concentrations. J. Biol. Chem. *277*, 36646–36655.

Chan, S.L., Mayne, M., Holden, C.P., Geiger, J.D., and Mattson, M.P. (2000). Presenilin-1 mutations increase levels of ryanodine receptors and calcium release in PC12 cells and cortical neurons. J. Biol. Chem. *275*, 18195–18200.

Cirrito, J.R., Yamada, K.A., Finn, M.B., Sloviter, R.S., Bales, K.R., May, P.C., Schoepp, D.D., Paul, S.M., Mennerick, S., and Holtzman, D.M. (2005). Synaptic activity regulates interstitial fluid amyloid-beta levels in vivo. Neuron *48*, 913–922.

Citron, M., Westaway, D., Xia, W., Carlson, G., Diehl, T., Levesque, G., Johnson-Wood, K., Lee, M., Seubert, P., Davis, A., et al. (1997). Mutant presenilins of Alzheimer's disease increase production of 42-residue amyloid beta-protein in both transfected cells and transgenic mice. Nat. Med. *3*, 67–72.

De Strooper, B. (2007). Loss-of-function presenilin mutations in Alzheimer disease. Talking point on the role of presenilin mutations in Alzheimer disease. EMBO Rep. *8*, 141–146.

Edbauer, D., Winkler, E., Regula, J.T., Pesold, B., Steiner, H., and Haass, C. (2003). Reconstitution of gamma-secretase activity. Nat. Cell Biol. *5*, 486–488.

Etcheberrigaray, R., Hirashima, N., Nee, L., Prince, J., Govoni, S., Racchi, M., Tanzi, R.E., and Alkon, D.L. (1998). Calcium responses in fibroblasts from asymptomatic members of Alzheimer's disease families. Neurobiol. Dis. *5*, 37–45.

Foskett, J.K., White, C., Cheung, K.H., and Mak, D.-O.D. (2007). Inositol trisphosphate receptor Ca^{2+} release channels. Physiol. Rev. *87*, 593–658.

Gandy, S., Doeven, M.K., and Poolman, B. (2006). Alzheimer disease: presenilin springs a leak. Nat. Med. *12*, 1121–1123.

Genazzani, A.A., Carafoli, E., and Guerini, D. (1999). Calcineurin controls inositol 1,4,5-trisphosphate type 1 receptor expression in neurons. Proc. Natl. Acad. Sci. USA *96*, 5797–5801.

Giacomello, M., Barbiero, L., Zatti, G., Squitti, R., Binetti, G., Pozzan, T., Fasolato, C., Ghidoni, R., and Pizzo, P. (2005). Reduction of Ca^{2+} stores and capacitative Ca^{2+} entry is associated with the familial Alzheimer's disease presenilin-2 T122R mutation and anticipates the onset of dementia. Neurobiol. Dis. *18*, 638–648.

Guo, Q., Furukawa, K., Sopher, B.L., Pham, D.G., Xie, J., Robinson, N., Martin, G.M., and Mattson, M.P. (1996). Alzheimer's PS-1 mutation perturbs calcium homeostasis and sensitizes PC12 cells to death induced by amyloid beta-peptide. Neuroreport *8*, 379–383.

Haass, C., and Selkoe, D.J. (2007). Soluble protein oligomers in neurodegeneration: lessons from the Alzheimer's amyloid beta-peptide. Nat. Rev. Mol. Cell Biol. *8*, 101–112.

Hardy, J. (2006). A hundred years of Alzheimer's disease research. Neuron *52*, 3–13.

Hardy, J., and Selkoe, D.J. (2002). The amyloid hypothesis of Alzheimer's disease: progress and problems on the road to therapeutics. Science *297*, 353–356.

Hebert, S.S., Serneels, L., Dejaegere, T., Horre, K., Dabrowski, M., Baert, V., Annaert, W., Hartmann, D., and De Strooper, B. (2004). Coordinated and widespread expression of gamma-secretase in vivo: evidence for size and molecular heterogeneity. Neurobiol. Dis. *17*, 260–272.

Hirashima, N., Etcheberrigaray, R., Bergamaschi, S., Racchi, M., Battaini, F., Binetti, G., Govoni, S., and Alkon, D.L. (1996). Calcium responses in human fibroblasts: a diagnostic molecular profile for Alzheimer's disease. Neurobiol. Aging *17*, 549–555.

Hutton, M., and Hardy, J. (1997). The presenilins and Alzheimer's disease. Hum. Mol. Genet. *6*, 1639–1646.

Ionescu, L., Cheung, K.H., Vais, H., Mak, D.O., White, C., and Foskett, J.K. (2006). Graded recruitment and inactivation of single $InsP_3$ receptor Ca^{2+}-release channels: implications for quantal Ca^{2+} release. J. Physiol. *573*, 645–662.

Ito, E., Oka, K., Etcheberrigaray, R., Nelson, T.J., McPhie, D.L., Tofel-Grehl, B., Gibson, G.E., and Alkon, D.L. (1994). Internal Ca^{2+} mobilization is altered in fibroblasts from patients with Alzheimer disease. Proc. Natl. Acad. Sci. USA *91*, 534–538.

Johnston, J.M., Burnett, P., Thomas, A.P., and Tezapsidis, N. (2006). Calcium oscillations in type-1 astrocytes, the effect of a presenilin 1 (PS1) mutation. Neurosci. Lett. *395*, 159–164.

Jolly-Tornetta, C., Gao, Z.Y., Lee, V.M., and Wolf, B.A. (1998). Regulation of amyloid precursor protein secretion by glutamate receptors in human Ntera 2 neurons. J. Biol. Chem. *273*, 14015–14021.

Kamenetz, F., Tomita, T., Hsieh, H., Seabrook, G., Borchelt, D., Iwatsubo, T., Sisodia, S., and Malinow, R. (2003). APP processing and synaptic function. Neuron *37*, 925–937.

Kasri, N.N., Kocks, S.L., Verbert, L., Hebert, S.S., Callewaert, G., Parys, J.B., Missiaen, L., and De Smedt, H. (2006). Up-regulation of inositol 1,4,5-trisphosphate receptor type 1 is responsible for a decreased endoplasmic-reticulum Ca^{2+} content in presenilin double knock-out cells. Cell Calcium *40*, 41–51.

LaFerla, F.M. (2002). Calcium dyshomeostasis and intracellular signalling in Alzheimer's disease. Nat. Rev. Neurosci. *3*, 862–872.

Laude, A.J., Tovey, S.C., Dedos, S.G., Potter, B.V., Lummis, S.C., and Taylor, C.W. (2005). Rapid functional assays of recombinant IP_3 receptors. Cell Calcium *38*, 45–51.

Leissring, M.A., Parker, I., and LaFerla, F.M. (1999a). Presenilin-2 mutations modulate amplitude and kinetics of inositol 1, 4,5-trisphosphate-mediated calcium signals. J. Biol. Chem. *274*, 32535–32538.

Leissring, M.A., Paul, B.A., Parker, I., Cotman, C.W., and LaFerla, F.M. (1999b). Alzheimer's presenilin-1 mutation potentiates inositol 1,4,5-trisphosphate-mediated calcium signaling in Xenopus oocytes. J. Neurochem. *72*, 1061–1068.

Leissring, M.A., Akbari, Y., Fanger, C.M., Cahalan, M.D., Mattson, M.P., and LaFerla, F.M. (2000). Capacitative calcium entry deficits and elevated luminal calcium content in mutant presenilin-1 knockin mice. J. Cell Biol. *149*, 793–798.

Leissring, M.A., LaFerla, F.M., Callamaras, N., and Parker, I. (2001). Subcellular mechanisms of presenilin-mediated enhancement of calcium signaling. Neurobiol. Dis. *8*, 469–478.

Lessard, C.B., Lussier, M.P., Cayouette, S., Bourque, G., and Boulay, G. (2005). The overexpression of presenilin2 and Alzheimer's-disease-linked presenilin2 variants influences TRPC6-enhanced Ca^{2+} entry into HEK293 cells. Cell. Signal. *17*, 437–445.

Mak, D.-O.D., McBride, S., and Foskett, J.K. (1998). Inositol 1,4,5-trisphosphate activation of inositol trisphosphate receptor Ca^{2+} channel by ligand tuning of Ca^{2+} inhibition. Proc. Natl. Acad. Sci. USA *95*, 15821–15825.

Mattson, M.P. (2004). Pathways towards and away from Alzheimer's disease. Nature *430*, 631–639.

Mattson, M.P., and Guo, Q. (1997). Cell and molecular neurobiology of presenilins: a role for the endoplasmic reticulum in the pathogenesis of Alzheimer's disease? J. Neurosci. Res. *50*, 505–513.

Mattson, M.P., and Chan, S.L. (2003). Neuronal and glial calcium signaling in Alzheimer's disease. Cell Calcium *34*, 385–397.

Mattson, M.P., Zhu, H., Yu, J., and Kindy, M.S. (2000). Presenilin-1 mutation increases neuronal vulnerability to focal ischemia in vivo and to hypoxia and glucose deprivation in cell culture: involvement of perturbed calcium homeostasis. J. Neurosci. *20*, 1358–1364.

McCormack, J.G., Halestrap, A.P., and Denton, R.M. (1990). Role of calcium ions in regulation of mammalian intramitochondrial metabolism. Physiol. Rev. *70*, 391–425.

Meberg, P.J., and Miller, M.W. (2003). Culturing hippocampal and cortical neurons. Methods Cell Biol. *71*, 111–127.

Nelson, O., Tu, H., Lei, T., Bentahir, M., de Strooper, B., and Bezprozvanny, I. (2007). Familial Alzheimer disease-linked mutations specifically disrupt Ca^{2+} leak function of presenilin 1. J. Clin. Invest. *117*, 1230–1239.

Oh, Y.S., and Turner, R.J. (2006). Effect of gamma-secretase inhibitors on muscarinic receptor-mediated calcium signaling in human salivary epithelial cells. Am. J. Physiol. Cell Physiol. *291*, C76–C82.

Querfurth, H.W., and Selkoe, D.J. (1994). Calcium ionophore increases amyloid beta peptide production by cultured cells. Biochemistry *33*, 4550–4561.

Scheuner, D., Eckman, C., Jensen, M., Song, X., Citron, M., Suzuki, N., Bird, T.D., Hardy, J., Hutton, M., Kukull, W., et al. (1996). Secreted amyloid beta-protein similar to that in the senile plaques of Alzheimer's disease is increased in vivo by the presenilin 1 and 2 and APP mutations linked to familial Alzheimer's disease. Nat. Med. *2*, 864–870.

Schneider, I., Reverse, D., Dewachter, I., Ris, L., Caluwaerts, N., Kuiperi, C., Gilis, M., Geerts, H., Kretzschmar, H., Godaux, E., et al. (2001). Mutant presenilins disturb neuronal calcium homeostasis in the brain of transgenic mice, decreasing the threshold for excitotoxicity and facilitating long-term potentiation. J. Biol. Chem. *276*, 11539–11544.

Shen, J., and Kelleher, R.J., 3rd. (2007). The presenilin hypothesis of Alzheimer's disease: evidence for a loss-of-function pathogenic mechanism. Proc. Natl. Acad. Sci. USA *104*, 403–409.

Smith, I.F., Boyle, J.P., Vaughan, P.F., Pearson, H.A., Cowburn, R.F., and Peers, C.S. (2002). Ca^{2+} stores and capacitative Ca^{2+} entry in human neuroblastoma (SH-SY5Y) cells expressing a familial Alzheimer's disease presenilin-1 mutation. Brain Res. *949*, 105–111.

Smith, I.F., Green, K.N., and LaFerla, F.M. (2005a). Calcium dysregulation in Alzheimer's disease: recent advances gained from genetically modified animals. Cell Calcium *38*, 427–437.

Smith, I.F., Hitt, B., Green, K.N., Oddo, S., and LaFerla, F.M. (2005b). Enhanced caffeine-induced Ca^{2+} release in the 3xTg-AD mouse model of Alzheimer's disease. J. Neurochem. *94*, 1711–1718.

Stutzmann, G.E. (2005). Calcium dysregulation, IP_3 signaling, and Alzheimer's disease. Neuroscientist *11*, 110–115.

Stutzmann, G.E., Caccamo, A., LaFerla, F.M., and Parker, I. (2004). Dysregulated IP3 signaling in cortical neurons of knock-in mice expressing an Alzheimer's-linked mutation in presenilin1 results in exaggerated Ca^{2+} signals and altered membrane excitability. J. Neurosci. *24*, 508–513.

Stutzmann, G.E., Smith, I., Caccamo, A., Oddo, S., Laferla, F.M., and Parker, I. (2006). Enhanced ryanodine receptor recruitment contributes to Ca^{2+} disruptions in young, adult, and aged Alzheimer's disease mice. J. Neurosci. *26*, 5180–5189.

Sugawara, H., Kurosaki, M., Takata, M., and Kurosaki, T. (1997). Genetic evidence for involvement of type 1, type 2 and type 3 inositol 1,4,5-trisphosphate receptors in signal transduction through the B-cell antigen receptor. EMBO J. *16*, 3078–3088.

Supnet, C., Grant, J., Kong, H., Westaway, D., and Mayne, M. (2006). Amyloid-beta-(1–42) increases ryanodine receptor-3 expression and function in neurons of TgCRND8 mice. J. Biol. Chem. *281*, 38440–38447.

Suzuki, N., Cheung, T.T., Cai, X.D., Odaka, A., Otvos, L., Jr., Eckman, C., Golde, T.E., and Younkin, S.G. (1994). An increased percentage of long amyloid beta protein secreted by familial amyloid beta protein precursor (beta APP717) mutants. Science *264*, 1336–1340.

Takeda, T., Asahi, M., Yamaguchi, O., Hikoso, S., Nakayama, H., Kusakari, Y., Kawai, M., Hongo, K., Higuchi, Y., Kashiwase, K., et al. (2005). Presenilin 2 regulates the systolic function of heart by modulating Ca^{2+} signaling. FASEB J. *19*, 2069–2071.

Tu, H., Nelson, O., Bezprozvanny, A., Wang, Z., Lee, S.F., Hao, Y.H., Serneels, L., De Strooper, B., Yu, G., and Bezprozvanny, I. (2006). Presenilins form ER Ca^{2+} leak channels, a function disrupted by familial Alzheimer's disease-linked mutations. Cell *126*, 981–993.

Verkhratsky, A. (2005). Physiology and pathophysiology of the calcium store in the endoplasmic reticulum of neurons. Physiol. Rev. *85*, 201–279.

White, C., Li, C., Yang, J., Petrenko, N.B., Madesh, M., Thompson, C.B., and Foskett, J.K. (2005). The endoplasmic reticulum gateway to apoptosis by Bcl-X_L modulation of the $InsP_3R$. Nat. Cell Biol. *7*, 1021–1028.

Yoo, A.S., Cheng, I., Chung, S., Grenfell, T.Z., Lee, H., Pack-Chung, E., Handler, M., Shen, J., Xia, W., Tesco, G., et al. (2000). Presenilin-mediated modulation of capacitative calcium entry. Neuron *27*, 561–572.

Zatti, G., Ghidoni, R., Barbiero, L., Binetti, G., Pozzan, T., Fasolato, C., and Pizzo, P. (2004). The presenilin 2 M239I mutation associated with familial Alzheimer's disease reduces Ca^{2+} release from intracellular stores. Neurobiol. Dis. *15*, 269–278.

Zatti, G., Burgo, A., Giacomello, M., Barbiero, L., Ghidoni, R., Sinigaglia, G., Florean, C., Bagnoli, S., Binetti, G., Sorbi, S., et al. (2006). Presenilin mutations linked to familial Alzheimer's disease reduce endoplasmic reticulum and Golgi apparatus calcium levels. Cell Calcium *39*, 539–550.